A CFD Analysis of the Effect of Ice and Snow Accretion on the Aerodynamic Behavior of Bridge Cables

Dwaipayan Sharma[1], Ahmed Abdelaal[2], Douglas Nims[1]

[1] *Department of Civil and Environmental Engineering, University of Toledo, Toledo, OH, USA.*
[2] *Department of Engineering Technology and Industrial Distribution, Texas A&M University, College Station, TX, USA*

Dwaipayan.Sharma@rockets.utoledo.edu, Ahmed.Abdelaal@tamu.edu, Douglas.Nims@utoledo.edu

Abstract— **Accretion of ice or snow over bridge cables can adversely influence the aerodynamic coefficients of the cables. Wind-induced vibration has been observed and reported on different cable-stayed bridges where atmospheric icing occurred, which can lead to cable fatigue and damage to cable attachments, and cause safety and serviceability issues. Also, the vibration of bridge cables with ice or snow accretion can lead to the mechanical breaking of the accretion medium which would result in the shedding of this frozen medium. In the present work, a computational fluid dynamics (CFD) study using ANSYS Fluent was conducted on a 2D model of a bridge cable with ice accretion to examine the effect of accretion profile, accretion thickness, and accretion surface roughness on the drag coefficient, lift coefficient, and vibration frequency of the bridge cable. In this study, six different accretion profiles were investigated where an elliptical profile was located at different angles around the cable and the results were compared to the cable with no accretion. Simulation results showed that the vortex shedding frequency of the cables with accretion decreased by up to 15%, while the drag and lift coefficients increased by up to 61% and 58%, respectively. Four different accretion thicknesses for one of the accretion profiles were studied in which the drag coefficient, lift coefficient, and vibration frequency for each case were obtained from the simulations. It was found that as the accretion thickness increases, the drag coefficient decreases by 20% and the lift coefficient decreases by 58%, while there was no significant change in the vibration frequency. It was also found that the drag coefficient decreases with the increase of the roughness height for the symmetrical accretion profile case. This study provides a better understanding of the effect of ice and snow accretion on the aerodynamic behaviour of cable-stayed bridges which can be a crucial factor in the future designs of bridges. Furthermore, the method used in this study can be a good tool to predict ice and snow shedding due to mechanical breaking.**

Keywords—***Wind-induced vibration, lift coefficient, drag coefficient, vortex shedding frequency, CFD, accretion profile, accretion thickness***

I. INTRODUCTION

Atmospheric icing is one of the natural hazards that can affect different structures such as bridges [1-6], power transmission lines [7-9], wind turbines [10-12], and telecommunication towers [13]. Cable-stayed bridges in the United States (U.S.) and the lower part of Canada are examples of the structures that are severely affected by this phenomenon since nearly 85% of them are located in areas where icing events were historically reported [1, 2, 4]. Atmospheric icing term is used to summarize all different types of formation of ice and snow in the atmosphere which can be categorized into precipitation icing, in-cloud icing, and hoar frost [14, 15]. Each type requires certain weather conditions that lead to the accretion of either ice or snow with different characteristics on structures. For example, ice accretion can be rime which forms at temperatures well below freezing when small diameters water droplets hit the surface of the structure, or it can be glaze ice which occurs at slightly below the freezing temperature where the impinged droplets partially freeze on the surface and the remaining water flow which can turn to icicles [16, 17].

The ice accumulates on the sheath or external surface of the stay. The sheath protects the internal high-strength wire strands from the elements and can be made of high-density polyethylene (HDPE), steel, stainless steel, or aluminium pipe. In a typical stay cable, a number of high-strength steel strands run parallelly inside a smooth pipe [18]. The parallel seven-wire strand system is most common in the U.S. and is used in almost 75% of its bridges [19]. Loads on the cable are the factor that determines the number of strands used in each stay cable. In addition to the structural strength, the vibration of the cable must be considered in the design of the stay cable.

Although ice accretion may not pose a threat to the static loading of the cable-stayed bridge structure, the formation of ice or snow can cause undesirable changes to the dynamic load due to the change in the aerodynamic characteristics of the cable. The vibration of stay cables is one of the most serious problems in bridge aerodynamics and can cause safety and serviceability issues in cable-stayed bridges [20]. Wind and rain-induced vibrations have been found to cause high amplitude vibrations which cause many structural damages [21]. This has led to modifications of some surfaces such as high-density polyethylene (HDPE) cable sheathing to reduce these effects [16, 22].

The formation of ice on the cables can change the cable's shape which would vary the flow characteristic and change the aerodynamic performance [17], and eventually, trigger wind-induced vibration with high amplitude. The vibration of stay cables may lead to cable rupture and fatigue which may ultimately lead to the bridge collapse [23]. Several studies were performed to understand the effect of the ice accretion on the aerodynamics characteristics and coefficients such as the drag and lift coefficients [14, 17, 24, 25]. These studies have shown that ice accretion on cables would cause changes in the aerodynamic behaviour of the bridge cables.

Several models were developed to determine the ice and snow thickness and the accretion weight [4, 26-30]. One of the

assumptions used in estimating the profile of the accretion was a simple cosine law that was observed in wind tunnel experiments and field observations which led to an elliptical accretion profile [4]. Determining the thickness, shape, and location of the accretion is important since they will have direct effects on the aerodynamics of the bridge cables. In addition, the ice and snow accretion would change the roughness of the cables, which in turn, would affect the flow characteristics around the cables as was observed in Trush et al. [31].

In the present work, a Computational Fluid Dynamics (CFD) study using ANSYS Fluent was conducted on a 2D model of a bridge cable with ice/snow accretion to examine the aerodynamic behaviour of the cables at different conditions. Six different accretion profiles were investigated where the elliptical profile was located at different angles around the cable and the results were compared to the cable with no accretion. For one of the accretion profiles, four different accretion thicknesses with the values of 12.5 mm, 25 mm, 50 mm, and 63.5 mm were studied. In addition, the surface roughness influence on the accretion was investigated. Aerodynamics coefficients, such as the vortex shedding frequency, lift, and drag, were obtained from the CFD simulations and compared to the clear cable with no accretion and to each other.

II. Methodology

Computational Fluid Dynamics (CFD) is a branch of fluid mechanics that uses numerical analysis and data structures to solve and analyse problems related to fluid flows, heat transfer, and associated phenomena such as chemical reactions. CFD is an extremely powerful technique in the simulation that involves fluid flows which also spans a wide range of application areas including aerodynamics of aircraft and vehicles, electrical engineering, chemical process, marine engineering, environmental engineering, meteorology, and biological engineering. There are many commercial CFD software used in engineering including ANSYS Fluent, one of the most commonly used software, which was used in this study.

A. Validation Case

Before running the CFD simulations for the cable with the ice or snow accretion, a validation was conducted on a simple 2D cylinder using the software and the results were compared to previous experimental and numerical studies available in the literature [32-35]. The computational domain used for all simulations has the dimensions of $25D \times 20D$ as suggested by Pang et al. [36] and Vacondio et al. [37], where D is the diameter of the cable. In this study, an average value of cable diameter $D = 0.25\ m$ was used. The inlet boundary is located at $10D$ upstream of the cable, the outlet boundary is located at $15D$ of the cable, and in the cross-stream direction, both top and bottom sides are located at $10D$ as shown in Fig. 1.

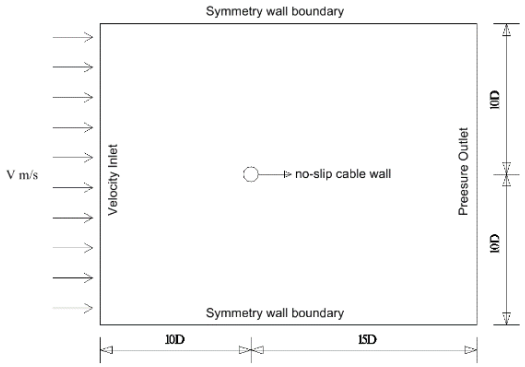

Fig. 1 Computation domain and boundary conditions for the 2D cylinder.

The mesh size around the boundary was 0.01 m with 50 inflation layers and the mesh size in the rest of the domain was set as 0.03 m. The edge sizing of 200 divisions was used around the cylinder. Fig. 2 shows the computation domain with meshing that was used for the simulation.

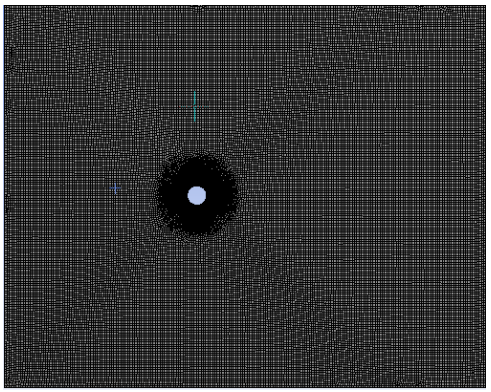

Fig. 2 Computation domain with meshing around the 2D cylinder.

Uniform inflow velocity is specified at the inlet and a moderate value of turbulence intensity (5%) was defined across the inlet boundary. The outlet boundary condition was assigned as a pressure outlet in which the flow that reaches the outlet was a fully developed unidirectional flow and the gauge pressure was zero. The upper and lower boundaries were assigned as symmetry boundary conditions. A "No-slip" condition for the velocity and a zero-gradient condition for pressure gradient was defined on the cylinder wall. The cylinder was assumed to be smooth with roughness height (K_s) of zero. The $k-\omega\ SST$ turbulence model was used as it covers a wide range of flow profiles with good accuracy [36]. PISO algorithm was used to solve the pressure-velocity coupling equations and a second-order upwind scheme was used for the spatial discretization of the simulations. The validations were conducted for two different Reynolds Numbers (Re); $Re = 100$ and $Re = 200$.

The values of the drag coefficient (C_d), lift coefficient (C_l), and Strouhal number (St) of the simulation were compared with the numbers from previous studies as shown in TABLE I. The drag and lift coefficients are dimensionless numbers used to measure the resistance and the lift on the object when it experiences fluid flow. The drag and lift coefficients can be calculated from Equations [1] and [2],

$$C_d = \frac{2F_d}{\rho V^2 A} \quad [1]$$

$$C_l = \frac{2F_l}{\rho V^2 A} \quad [2]$$

where F_d is the drag force, F_l is the lift force, ρ is the density of the fluid, V is the free stream velocity, and A is the frontal area of the cylinder.

The Strouhal number is a dimensionless parameter relevant to vortex excitation, which is the ratio of inertial forces due to local acceleration to the inertial force due to convective acceleration of the flow, which can be calculated using the following equation,

$$St = \frac{fd}{V} \quad [3]$$

where f is the frequency of vortex shedding in Hz and d is the cable diameter. Strouhal number (St) plays an important role in the calculation of wind velocity at which oscillation due to vortex shedding occurs.

TABLE I. COMPARISON OF SIMULATION RESULTS WITH PREVIOUS STUDIES

Results	$Re = 100$			$Re = 200$		
	C_d	C_l	St	C_d	C_l	St
Linnick and Fasel [32]	1.34	0.33	0.166	1.34	0.69	0.197
Herfjord [34]	1.36	0.34	0.168	1.35	0.70	0.196
Xu and Wang [35]	1.42	0.34	0.171	1.42	0.66	0.202
Present Study	1.46	0.40	0.172	1.32	0.64	0.198

As shown in TABLE I, the discrepancy between the simulation results and the previous studies varies across the drag coefficient (C_d), the lift coefficient (C_l), and the Strouhal number (St). The value discrepancies also differ for both Reynolds number cases. The average discrepancy in the value of the drag coefficient is 6% for $Re = 100$ and 3.8% for $Re = 200$, while the discrepancy in the value of the lift coefficient is 15.6% for $Re = 100$ and 6.77% for $Re = 200$. From these results, it can be noted that the discrepancies decreased for the higher Reynolds number which could be related to the flow behaviour. The Strouhal number average discrepancy is 2.1% for $Re = 100$ and 1.2% for $Re = 200$, which shows that the results of the simulations are in good agreement with the previous studies' data. Fig. 3 and Fig. 4 show the time-history plot of the drag coefficient (C_d) and lift coefficient (C_l) at $Re = 100$ and Power Spectral Density (PSD) of lift coefficient (C_l) at $Re = 100$, respectively.

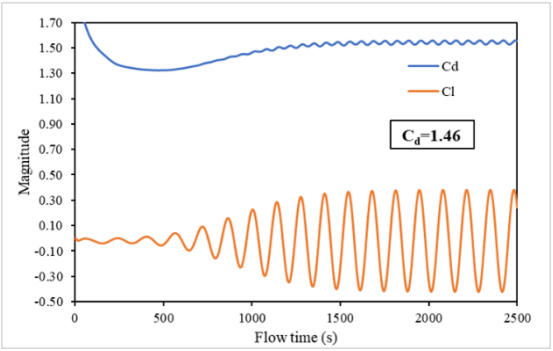

Fig. 3 Time-history plot of C_d and C_l at $Re = 100$.

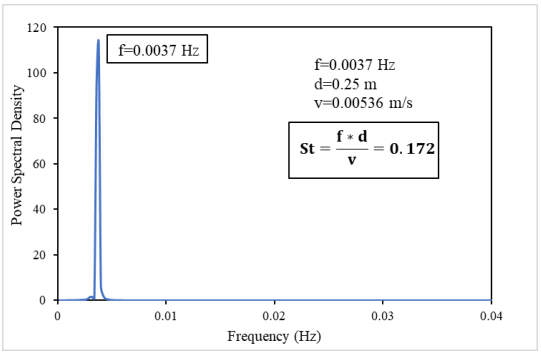

Fig. 4 Power Spectral Density (PSD) of C_l at $Re = 100$.

B. *Configuration and Numerical Model*

The simulation model was set up with the focus to study the wind flow around the ice accreted bridge cable. Similar to the validation case discussed earlier, the computation domain has the dimensions of $25D \times 20D$ as shown in Fig. 1, where the diameter of the cable (D) was taken to be $0.25\,m$. The accretion shape followed the cosine law assumption [4], which led to the presence of an elliptical thick ice layer on the windward side of the cable as shown in Fig. 5. Six different profiles were considered for this study in which the elliptical profile was located at different angles with respect to the wind direction in addition to the clear cylinder case. Fig. 6 shows the profiles where each profile was given cross-section numbers from 2 to 7 and the clear cylinder was given cross-section number 1. In addition, four different thicknesses of ice accretion were used for cross-section number 2 to study the influence of Various thicknesses. Also, three different roughness heights were applied to cross-section 2 for one of the thicknesses.

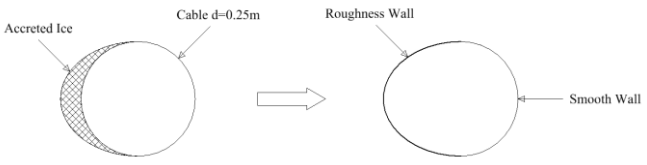

Fig. 5 Cable cross-section with ice/snow accretion covering windward side following the cosine law.

The boundary conditions were similar to the validation case, however, the inlet velocity was taken as $5\,m/s$, a typical wind speed for an ice storm, which changed the Reynolds number (Re) to 93,262.

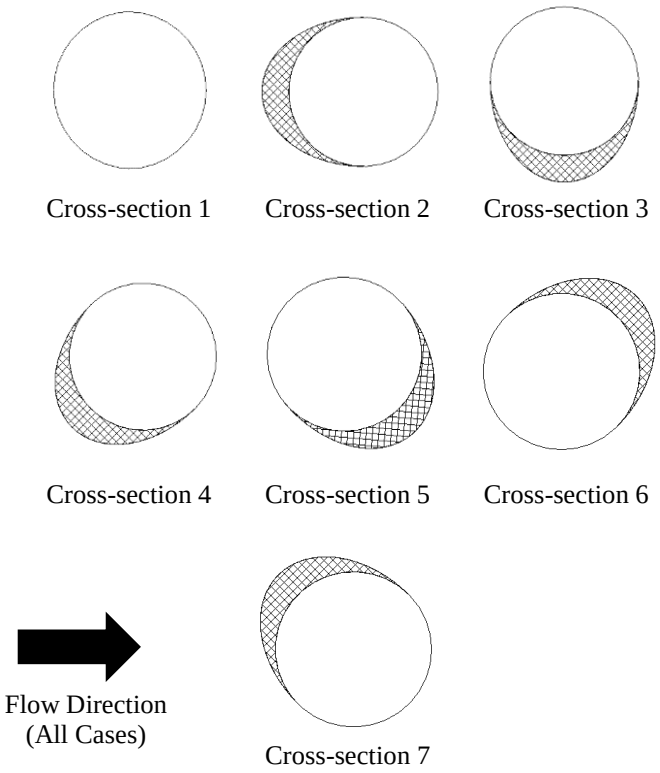

Fig. 6 Cable cross-sections used in the CFD simulations where cross-section 1 represents a clear cylinder and cross-sections 2 to 7 show cylinders with ice/snow accretion at different locations. The arrow shows the flow direction for all cases.

To obtain better results, inflation and edge sizing were used on the wall of the cylinder to define structured mesh where the circumference of the cylinder was evenly divided into 200 divisions in edge sizing. Quadrilateral elements were defined around the cylinder boundary, and triangular elements were defined in the outer zone to optimize the computation time and accuracy. Fig. 7 shows the meshing near the cylinder surface.

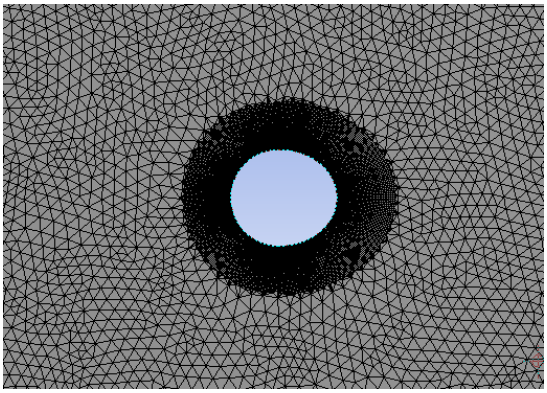

Fig. 7 Mesh near the cylinder with inflation and edge sizing.

Similar to the validation case, the $k-\omega\ SST$ turbulence model was used, PISO algorithm was used to solve the pressure-velocity coupling equations, and the second-order upwind scheme was used for the spatial discretization. TABLE II summarizes the computation conditions that were used for the simulations.

TABLE II. COMPUTATION CONDITIONS FOR THE SIMULATION

Diameter of cable	$0.25m$
Fluid Material	Air
Simulation Type	Transient Simulation
Temperature	$273\ K$
Wind Speed	$5\ m/s$
Kinematic Viscosity	$1.338 * 10^{-5}\ m^2/s$
Reynolds Number	93,262
Turbulence Model	$K-\omega\ SST$
Algorithm for Pressure-Velocity coupling equations	PISO Algorithm
Interpolating schemes	
Momentum	Second-order upwind
Turbulent kinetic energy	Second-order upwind
Turbulent dissipation rate	Second-order upwind
Time-dependent solution formulation	Second-order implicit
Boundary Conditions	
Inlet	Velocity Inlet
Outlet	Pressure Outlet
Upper and lower wall	Symmetry
Cable wall	No-slip condition

III. RESULTS AND DISCUSSION

In this study, three different parameters were considered to determine their effects on the aerodynamics performance which include the location of the accretion profile, the accretion thickness, and the accretion roughness. The accretion thickness was taken as 25 mm for the simulations that examine the effect of the location of the accretion; whereas for the effect of the thickness study, four different thicknesses were considered in the simulations including 12.5 mm, 25 mm, 50 mm, and 63.5 mm, and each was applied only to cross-section 2. For the influence of the accretion roughness, three different roughness heights (K_s) of 5 mm, 10 mm, and 15 mm were used on cross-section 2 where the roughness was assumed uniform by setting the roughness constant (C_s) as 0.5 in ANSYS Fluent. Results of these study cases are presented in the following sections.

A. Effect of Accretion Location on Bridge Cables Aerodynamic Performance

Initially, the simulation was run for the clear cylinder (cross-section 1) to determine the aerodynamics coefficients, i.e., drag coefficient (C_d), lift coefficient (C_l), vortex-shedding frequency (f), and Strouhal number (St). Then, the simulations were run for the other six profiles with accretion (cross-sections 2 to 7). Finally, the results of the six cases were compared to the clear cylinder case and each other.

Fig. 8 shows the results of the clear cylinder study (cross-section 1). As shown in the figure, the drag coefficient, lift coefficient, frequency, and Strouhal number obtained from the simulation were: 0.93, -1.2 to 1.2, 5.2 Hz, and 0.26, respectively. The simulation results of the other six cases are shown in TABLE III. Fig. 9 shows the results of one of the six cases with ice accretion (cross-section 3).

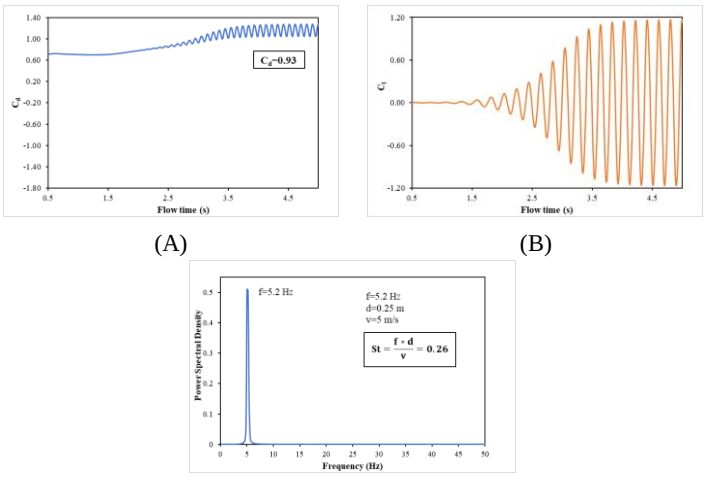

(A) (B)

(C)

Fig. 8 Simulation results of the clear cylinder (cross-section 1) with no accretion where A) drag coefficient vs flow time, B) lift coefficient vs flow time, and C) PSD of lift coefficient vs frequency are displayed.

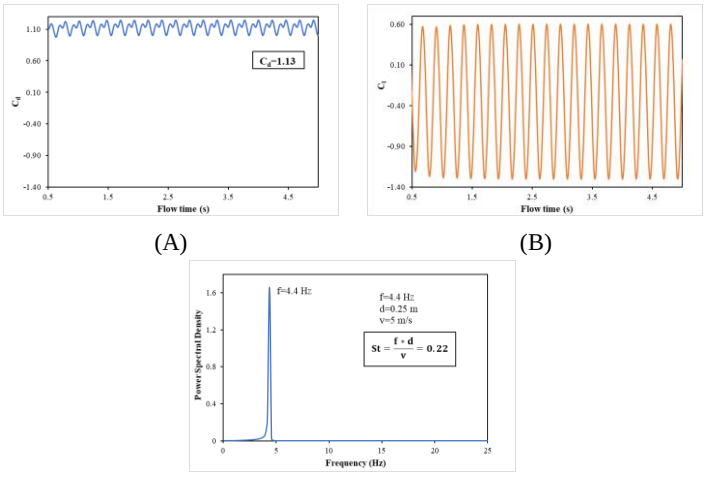

(A) (B)

(C)

Fig. 9 Simulation results of the cylinder with ice/snow accretion (cross-section 3) where A) drag coefficient vs flow time, B) lift coefficient vs flow time, and C) PSD of lift coefficient vs frequency are displayed.

TABLE III. Comparison of drag coefficient, lift coefficient, frequency, and Strouhal number for different cable cross-sections

Cross-section	C_d	C_l	$f(Hz)$	St
1(Clear)	0.93	-1.20 to 1.20	5.2	0.26
2	1.03	-1.45 to 1.45	5.0	0.25
3	1.13	-1.30 to 0.60	4.4	0.22
4	1.17	-1.70 to 0.70	4.4	0.22
5	1.29	-1.40 to 1.10	4.4	0.22
6	1.50	-1.35 to 1.80	4.4	0.22
7	1.48	-1.40 to 1.90	4.4	0.22

As shown in TABLE III, the drag coefficients for the cables with accretion were higher than the clear surface. The drag coefficient increases from nearly 10% for cross-section 2 to 61% for cross-section 6 case which had the highest drag. The change in the drag coefficient is related to the mechanism of how the air flows around the cylinder. For the lift coefficient, the coefficient value oscillates about $y = 0$ (X-axis) for the clear cylinder case and cross-section 2 where the accretion was facing the windward side. However, the lift coefficient oscillates about either a positive y value or negative y value instead of $y = 0$ as in the rest of the cases due to the asymmetric shape of the cylinder with accretion compared to the first two cases. Considering the maximum values of the lift coefficients for all cases in comparison to the clear cable, the lift coefficient increased by nearly 58% for cross-section 7. It can also be seen from the above simulation results that the vibration frequency and the Strouhal numbers were maximum for the clear cable (cross-section 1) but decreased for the cables with accretion cases by 4% in the cross-section 2 case and by nearly 15% in the rest of the cases.

B. Effect of Accretion Thickness on Bridge Cables Aerodynamic Performance

To assess the effect of the accretion thickness on the bridge cable aerodynamic characteristics, simulations were performed for one of the above-discussed cases (cross-section 2) with four different thicknesses: 12.5 mm, 25 mm, 50 mm, and 63.5 mm. This case was considered since generally, the wind would be blowing on the windward side where ice accretion was located. As was done in the previous cases, the drag coefficient (C_d), lift coefficient (C_l), vortex-shedding frequency (f), and Strouhal number (St) were obtained from the simulations and were used for comparison. Fig. 10 shows the simulation results for one of the cases (thickness of 12.5 mm) and TABLE IV shows the results of all the cases.

TABLE IV. Comparison of drag coefficient, lift coefficient, frequency, and Strouhal number for different accreted ice thickness

Accretion Thickness	C_d	C_l	$f(Hz)$	St
0 mm	0.93	-1.20 to 1.20	5.2	0.26
12.5 mm	1.16	-1.5 to 1.5	4.8	0.24
25 mm	1.03	-1.45 to 1.45	5	0.25
50 mm	0.82	-1 to 1	5	0.25
63.5 mm	0.74	-0.5 to 0.5	5	0.25

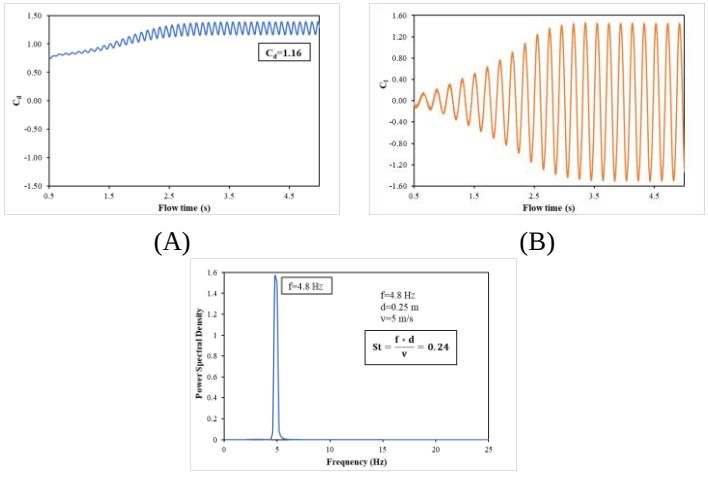

(A) (B)

(C)

Fig. 10 Simulation results of the cylinder with ice/snow accretion (cross-section 2) with a thickness of 12.5 mm where A) drag coefficient vs flow time, B) lift coefficient vs flow time, and C) PSD of lift coefficient vs frequency are displayed.

As presented in TABLE IV, the drag coefficient decreases as the thickness of the accreted ice increases, which was also observed in previous studies [38]. In addition, the range of lift coefficient decreases as the ice thickness increases. The drag coefficient decreased by 20% and the lift coefficient decreased by 58% for the accretion thickness of 63.5 mm. The decrease in the drag coefficient is believed to be due to the streamlining of the cable profile with accretion. The frequency and Strouhal number did not change significantly from the clear cable and were constant from thickness 25 mm and higher.

C. *Effect of Accretion Roughness on Bridge Cables Aerodynamic Performance*

Surface roughness is one of the crucial parameters that can affect the aerodynamics behaviour of bridge cables. To study the effect of accretion roughness on the aerodynamic coefficients of the cables, three different roughness heights (K_s) of 5 mm, 10 mm, and 15 mm were applied to cross-section 2 with an accretion thickness of 25 mm. Similarly, the drag coefficient (C_d), lift coefficient (C_l), vortex-shedding frequency (f), and Strouhal number (St) were obtained from ANSYS Fluent for all cases. Fig. 11 shows the simulation results for one of the roughness heights ($K_s = 5mm$) and TABLE V shows the results of all cases.

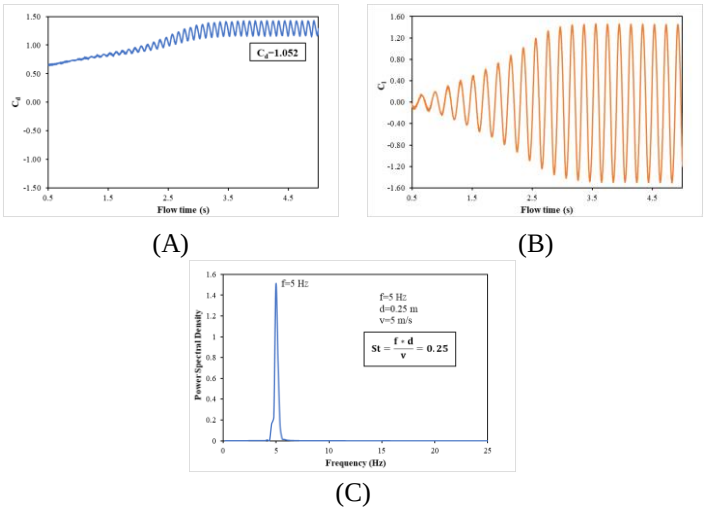

(A) (B)

(C)

Fig. 11 Simulation results of the cylinder with ice/snow accretion (cross-section 2) with a thickness of 25 mm and surface roughness of 5 mm where A) drag coefficient vs flow time, B) lift coefficient vs flow time, and C) PSD of lift coefficient vs frequency are displayed.

TABLE V. Comparison of drag coefficient, frequency, and Strouhal number for different accretion roughness for cross-section 2 with a thickness of 25 mm

Roughness height (Ks)	C_d	C_l	$f(Hz)$	St
0 mm	1.03	-1.45 to 1.45	5	0.25
5 mm	1.052	-1.45 to 1.45	5	0.25
10 mm	1.04	-1.45 to 1.45	5	0.25
15 mm	1.035	-1.45 to 1.45	5	0.25

As can be seen in TABLE V, the accretion roughness increased the drag coefficient in comparison to the original case with no roughness. Also, as shown in this table, the drag coefficient value decreases with the increase in roughness height (K_s). Roughness height had no impact on the vortex shedding frequency and Strouhal number which is expected since the roughness is uniform. For the same reason, the lift coefficient value was the same and the mean value of the lift coefficient oscillates around $y = 0$ for all cases.

IV. Conclusions

This work utilized a CFD approach to study the aerodynamic performance and vibration frequency of cable with a simplified elliptical ice/snow accretion shape following the cosine law. The study aimed to understand the effect of the accretion location, the thickness, and the accretion roughness on the drag coefficient (C_d), lift coefficient (C_l), vortex-shedding frequency (f), and Strouhal number (St) by using ANSYS Fluent. The important findings of this study can be summarized in the following points:

- The cable section with ice accretion has a higher value of drag coefficient than clear cylindrical cable with no ice accretion. The drag coefficient of the iced cable section increased by up to 61% from the clear cable.
- Cable with no ice accretion and with symmetrical ice accretion by taking the wind direction into account have the lift coefficient oscillates around $y = 0$. For the cable with asymmetrical accretion, the lift coefficient oscillates either about positive y value or negative y value depending on the location of the accretion. The lift coefficient of iced cable increased by up to 58%.
- The maximum percentage change in the value of vibration frequency (f) due to icing accretion location was 15.4%.
- As the thickness of accretion increases, both the drag coefficient value and the range lift coefficient decrease. The drag coefficient decreased by 20% and the lift coefficient decreased by 58% in this study.

With the increase in the roughness height (Ks), the value of the drag coefficient decreases. The roughness height has no impact on the vibration frequency (f) of ice accreted cable section. This study shows that the location of the ice accretion had some effects on the aerodynamics forces acting on the cables. Both the drag and lift coefficients increased with the change of the accretion location which can cause more stress on the cables and shorter fatigue life. Although there were no significant changes in the cable vibration frequency due to icing, it is believed that for different accretion profiles, more changes can occur in the frequency. The change in the accretion thickness was conducted for only one of the profiles that had symmetrical accretion where the accretion was facing the wind. For this case, the drag and lift coefficients decreased with the increase of the thickness due to the streamlining of the profile and there were no significant changes in the vibration frequency. However, this could also change if another accretion location was considered. Moreover, the change of the ice roughness for the symmetrical case (cross-section 2) was found to increase the drag coefficient which decreases as the roughness height increases, but it was found to have minimal to no effect on lift coefficient, vortex shedding frequency, and Strouhal number. However, it may differ if a different profile was considered, or the roughness

was not uniform. In addition to affecting the fatigue life of the bridge cables, these changes in aerodynamics behaviours and frequency may lead to mechanical breaking of the accretion medium. This would result in the shedding of the frozen medium. Ice or snow shedding from bridge cables can be a serious problem to the public and bridge operators as it affects public safety in addition to causing economic losses.

V. References

[1] D. K. Nims, V. Hunt, A. Helmicki, and T.-M. Ng, "Ice Prevention or Removal on the Veteran's Glass City Skyway Cables Final Report," Ohio Department of Transportation Office of Research and Development, State Job Number 134489, 2014.

[2] C. Mirto, A. Abdelaal, D. K. Nims, T.-M. Ng, V. Hunt, A. Helmicki, C. Ryerson, and K. Jones, "Icing Management on the Veterans' Glass City Skyway Stay Cables," *Transportation Research Record: Journal of the Transportation Research Board*, vol. 2482, no. 1, pp. 74-81, 2015, doi: https://doi.org/10.3141/2482-10.

[3] K. Kleissl and C. T. Georgakis, "Bridge ice accretion and de- and anti-icing systems: A review," in *The 7th Internation Cable Supported Bridge Operators' Conference*, Jiangsu, China, 2010, pp. 161-167.

[4] A. Abdelaal, D. Nims, K. Jones, and H. Sojoudi, "Prediction of ice accumulation on bridge cables during freezing rain: A theoretical modeling and experimental study," *Cold Regions Science and Technology*, vol. 164, p. 102782, 2019/08/01/ 2019, doi: https://doi.org/10.1016/j.coldregions.2019.102782.

[5] J. Andre, A. Kiremidjian, and C. T. Georgakis, "Statistical Modeling of Time Series for Ice Accretion Detection on Bridge Cables," *Journal of Cold Regions Engineering*, vol. 32, no. 2, p. 04018004, 2018, doi: https://doi.org/10.1061/(ASCE)CR.1943-5495.0000157.

[6] A. Abdelaal, C. Mirto, D. K. Nims, T.-M. Ng, K. Jones, C. Ryerson, A. Helmicki, and V. Hunt, "Investigation of using icephobic coatings on a Cable Stayed Bridge," in *IWAIS 2015. Proceedings of the 16th International Workshop on Atmospheric Icing of Structures*, 2015.

[7] K. Savadjiev and M. Farzaneh, "Modeling of icing and ice shedding on overhead power lines based on statistical analysis of meteorological data," *IEEE Transactions on Power Delivery*, vol. 19, no. 2, pp. 715-721, 2004, doi: https://doi.org/10.1109/TPWRD.2003.822527.

[8] T. Ishihara and S. Oka, "A numerical study of the aerodynamic characteristics of ice-accreted transmission lines," *Journal of Wind Engineering and Industrial Aerodynamics*, vol. 177, pp. 60-68, 2018/06/01/ 2018, doi: https://doi.org/10.1016/j.jweia.2018.04.008.

[9] B. Liu, K. Ji, X. Zhan, X. Fei, P. Li, B. Zhao, Y. Dong, C. Deng, L. Liu, Z. Wang, Y. Luo, and Y. Bai, "Experimental and numerical analysis of overhead transmission lines vibration due to atmospheric icing," in *2017 Prognostics and System Health Management Conference (PHM-Harbin)*, 9-12 July 2017 2017, pp. 1-4, doi: https://doi.org/10.1109/PHM.2017.8079288.

[10] M. C. Homola, P. J. Nicklasson, and P. A. Sundsbø, "Ice sensors for wind turbines," *Cold Regions Science and Technology*, vol. 46, no. 2, pp. 125-131, 2006/11/01/ 2006, doi: https://doi.org/10.1016/j.coldregions.2006.06.005.

[11] L. Gao, Y. Liu, W. Zhou, and H. Hu, "An experimental study on the aerodynamic performance degradation of a wind turbine blade model induced by ice accretion process," *Renewable Energy*, vol. 133, pp. 663-675, 2019/04/01/ 2019, doi: https://doi.org/10.1016/j.renene.2018.10.032.

[12] Y. Han, J. Palacios, and S. Schmitz, "Scaled ice accretion experiments on a rotating wind turbine blade," *Journal of Wind Engineering and Industrial Aerodynamics*, vol. 109, pp. 55-67, 2012/10/01/ 2012, doi: https://doi.org/10.1016/j.jweia.2012.06.001.

[13] N. D. Mulherin, "Atmospheric icing and communication tower failure in the United States," *Cold Regions Science and Technology*, vol. 27, no. 2, pp. 91-104, 1998/04/01/ 1998, doi: https://doi.org/10.1016/S0165-232X(97)00025-6.

[14] C. Demartino, H. Koss, C. Georgakis, and F. Ricciardelli, "Effects of ice accretion on the aerodynamics of bridge cables," *Journal of Wind Engineering and Industrial Aerodynamics*, vol. 138, 03/31 2015, doi: https://doi.org/10.1016/j.jweia.2014.12.010.

[15] M. Farzaneh, *Atmospheric icing of power networks*. Springer Science & Business Media, 2008.

[16] Y. Liu, W. Chen, Y. Peng, and H. Hu, "An experimental study on the dynamic ice accretion processes on bridge cables with different surface modifications," *Journal of Wind Engineering and Industrial Aerodynamics*, vol. 190, pp. 218-229, 2019/07/01/ 2019, doi: https://doi.org/10.1016/j.jweia.2019.05.007.

[17] H. H. Koss, H. Gjelstrup, and C. T. Georgakis, "Experimental study of ice accretion on circular cylinders at moderate low temperatures," *Journal of Wind Engineering and Industrial Aerodynamics*, vol. 104-106, pp. 540-546, 2012/05/01/ 2012, doi: https://doi.org/10.1016/j.jweia.2012.03.024.

[18] M. Ito, "Stay Cable Technology: Overview.," in *International Association for Bridge and Structural Engineering (IABSE)*, Malmo, Sweden, 1999, pp. 481-490.

[19] National Cooperative Highway Research Program (NCHRP), "Inspection and Maintenance of Bridge Stay Cable Systems," Transportation Research Board 2005. [Online]. Available: https://www.trb.org/publications/nchrp/nchrp_syn_353.pdf

[20] M. Matsumoto, H. Shirato, T. Yagi, M. Goto, S. Sakai, and J. Ohya, "Field observation of the full-scale wind-induced cable vibration," *Journal of Wind Engineering and Industrial Aerodynamics*, vol. 91, no. 1, pp. 13-26, 2003/01/01/ 2003, doi: https://doi.org/10.1016/S0167-6105(02)00332-X.

[21] Y. Hikami and N. Shiraishi, "Rain-wind induced vibrations of cables stayed bridges," *Journal of Wind Engineering and Industrial Aerodynamics*, vol. 29, no. 1, pp. 409-418, 1988/08/01/ 1988, doi: https://doi.org/10.1016/0167-6105(88)90179-1.

[22] K. Kleissl and C. T. Georgakis, "Comparison of the aerodynamics of bridge cables with helical fillets and a pattern-indented surface," *Journal of Wind Engineering and Industrial Aerodynamics*, vol. 104-106, pp. 166-175, 2012/05/01/ 2012, doi: https://doi.org/10.1016/j.jweia.2012.02.031.

[23] D. Zuo, N. P. Jones, and J. A. Main, "Field observation of vortex- and rain-wind-induced stay-cable vibrations in a three-dimensional environment," *Journal of Wind Engineering and Industrial Aerodynamics*, vol. 96, no. 6, pp. 1124-1133, 2008/06/01/ 2008, doi: https://doi.org/10.1016/j.jweia.2007.06.046.

[24] H. Gjelstrup, C. T. Georgakis, and A. Larsen, "An evaluation of iced bridge hanger vibrations through wind tunnel testing and quasi-steady theory," *Wind and Structures*, vol. 15, no. 5, pp. 385-407, 2012, doi: https://doi.org/10.12989/was.2012.15.5.385.

[25] P. Górski, M. Tatara, S. Pospíšil, and A. Trush, "Aerodynamic force coefficients of an ice-accreted bridge cable in low and moderately turbulent wind," *Journal of Wind Engineering and Industrial Aerodynamics*, vol. 205, p. 104335, 2020/10/01/ 2020, doi: https://doi.org/10.1016/j.jweia.2020.104335.

[26] L. Makkonen, "Modeling power line icing in freezing precipitation," *Atmospheric Research*, vol. 46, no. 1, pp. 131-142, 1998/04/01/ 1998, doi: https://doi.org/10.1016/S0169-8095(97)00056-2.

[27] K. F. Jones, "A simple model for freezing rain ice loads," *Atmospheric Research*, vol. 46, no. 1, pp. 87-97, 1998/04/01/ 1998, doi: https://doi.org/10.1016/S0169-8095(97)00053-7.

[28] L. Makkonen, "Models for the growth of rime, glaze, icicles and wet snow on structures," *Philosophical Transactions of the Royal Society of London. Series A: Mathematical, Physical and Engineering Sciences*, vol. 358, no. 1776, pp. 2913-2939, 2000, doi: https://doi.org/10.1098/rsta.2000.0690.

[29] B. E. K. Nygaard, H. Ágústsson, and K. Somfalvi-Tóth, "Modeling Wet Snow Accretion on Power Lines: Improvements to Previous Methods Using 50 Years of Observations," (in English), *Journal of Applied Meteorology and Climatology*, vol. 52, no. 10, pp. 2189-2203, 01 Oct. 2013 2013, doi: https://doi.org/10.1175/JAMC-D-12-0332.1.

[30] A. Abdelaal, "Atmospheric Icing on Bridge Stays," Ph.D. Ph.D. Dissertation, University of Toledo, 2016. [Online]. Available: http://rave.ohiolink.edu/etdc/view?acc_num=toledo1483746010505796

[31] A. Trush, S. Pospíšil, S. Kuznetsov, and H. Kozmar, "Wind-Tunnel Experiments on Vortex-Induced Vibration of Rough Bridge Cables," *Journal of Bridge Engineering*, vol. 22, no. 10, p. 06017001, 2017, doi: https://doi.org/10.1061/(ASCE)BE.1943-5592.0001104.

[32] M. N. Linnick and H. F. Fasel, "A high-order immersed interface method for simulating unsteady incompressible flows on irregular domains," *Journal of Computational Physics*, vol. 204, no. 1, pp. 157-192, 2005, doi: https://doi.org/10.1016/j.jcp.2004.09.017.

[33] D. Russell and Z. Jane Wang, "A cartesian grid method for modeling multiple moving objects in 2D incompressible viscous flow," *Journal of Computational Physics*, vol. 191, no. 1, pp. 177-205, 2003/10/10/ 2003, doi: https://doi.org/10.1016/S0021-9991(03)00310-3.

[34] K. Herfjord, "A study of two-dimensional separated flow by a combination of the finite element method and Navier-Stokes equations," Doctoral, Department of Marine Hydrodynamics, , The Norwegian Institute of Technology, University of Trondheim, Trondheim, Norway., 1996. [Online]. Available: https://repository.tudelft.nl/islandora/object/uuid:b59396e3-0368-428c-8481-d9f8ceb60f25

[35] S. Xu and Z. J. Wang, "An immersed interface method for simulating the interaction of a fluid with moving boundaries," *Journal of Computational Physics*, vol. 216, no. 2, pp. 454-493, 2006/08/10/ 2006, doi: https://doi.org/10.1016/j.jcp.2005.12.016.

[36] A. L. J. Pang, M. Skote, and S.-Y. Lim, "Modelling high Re flow around a 2D cylindrical bluff body using the k0É (SST) turbulence model," *Progress in Computational Fluid Dynamics*, vol. 16, no. 1, pp. 48-57, 2016, doi: http://dx.doi.org/10.1504/PCFD.2016.074225.

[37] R. Vacondio, B. D. Rogers, P. K. Stansby, P. Mignosa, and J. Feldman, "Variable resolution for SPH: A dynamic particle coalescing and splitting scheme," *Computer Methods in Applied Mechanics and Engineering*, vol. 256, pp. 132-148, 2013/04/01/ 2013, doi: https://doi.org/10.1016/j.cma.2012.12.014.

[38] S. Li, T. Wu, T. Huang, and Z. Chen, "Aerodynamic stability of iced stay cables on cable-stayed bridge," *Wind and Structures*, vol. 23, no. 3, pp. 253-273, 09/25 2016, doi: https://doi.org/10.12989/was.2016.23.3.253.